This is a repository copy of *Permanent-magnet brushless machines with unequal tooth widths and similar slot and pole numbers* .

White Rose Research Online URL for this paper:
http://eprints.whiterose.ac.uk/862/

Article:

eprints@whiterose.ac.uk
https://eprints.whiterose.ac.uk/

Permanent-Magnet Brushless Machines With Unequal Tooth Widths and Similar Slot and Pole Numbers

Dahaman Ishak, Z. Q. Zhu, *Senior Member, IEEE*, and David Howe

Abstract—This paper presents a comparative study of three-phase permanent-magnet brushless machines in which the slot and pole numbers are similar, with reference to conventional brushless dc machines in which the ratio of the slot number to pole number is usually $3:2$. Three different motor designs are considered. Two have equal tooth widths, with one having a coil wound on every tooth and the other only having a coil wound on alternate teeth, while the third machine also has coils wound on alternate teeth but these are wider than the unwound teeth while the width of their tooth tips is almost equal to the rotor pole pitch in order to maximize the flux linkage and torque. Analytical and finite-element methods are employed to predict the flux-linkage and back-electromotive-force waveforms, and the self- and mutual-inductances, and these are shown to be in good agreement with measured results. It is also shown that the third machine is eminently appropriate for brushless dc operation.

Index Terms—Back electromotive force (EMF), brushless machines, flux linkage, fractional slot, permanent magnet.

I. INTRODUCTION

IN ORDER to maximize the efficiency and torque density of permanent-magnet brushless machines, nonoverlapping stator windings are often employed since they result in shorter end windings and, hence, a lower copper loss and a shorter overall axial length [1], [2]. Further, developments for safety critical applications, such as flight control surface actuation in "more-electric" aircraft, have resulted in machines with a high degree of fault tolerance [3]–[5]. Such machines, in addition to having a higher number of phases, only have alternate teeth wound, and are often referred to as modular permanent-magnet machines [6], and make it easier to realize a high per-unit self-inductance.

The three-phase permanent-magnet brushless machines which are investigated in this paper also employ nonoverlapping windings, while their slot number and pole number are similar, in that they only differ by two. Machine designs in which all the teeth and only alternate teeth carry a coil are considered, and in the latter case the benefit of making the

coil pitch approximately equal to a pole pitch, by employing unequal tooth widths for the wound and unwound teeth and making the tooth tips of the wound teeth span approximately one pole pitch, is investigated [7], [8].

The electromagnetic performance of the three machine designs, having 12 slots and ten poles and a rated torque of 5.5 N·m at 400 r/min, is predicted by analytical and finite-element methods, the predictions being validated by measurements.

II. MACHINES WITH UNEQUAL TOOTH WIDTHS AND SIMILAR SLOT AND POLE NUMBERS

Clearly, it is desirable for the coil pitch to be as close to the pole pitch as is feasible in order to maximize the flux linkage and torque density. Therefore, the number of slots (N_s) and poles $(2p)$ should differ by the smallest possible integer. The closest slot and pole number combinations are related by $2p = N_s \pm 1$, i.e., the slot number and pole number differ only by one. However, such machines would inherently exhibit unbalanced magnetic pull, and may result in excessive noise and vibration. Hence, in practice, the most appropriate slot and pole numbers are related by $2p = N_s \pm 2$. The merits of such slot number/pole number combinations have been discussed elsewhere by the authors [9], [10]. For a balanced three-phase machine, typical $N_s/2p$ combinations are 6/4, 6/8; 12/10, 12/14; 18/16, 18/20; 24/22, 24/26, etc. In such machines either all the teeth or only alternate teeth can carry a coil, as illustrated in Fig. (1a) and (b), respectively [9]. The electromagnetic performance, in terms of the back electromotive force (EMF), the cogging torque, and the winding inductances, of machines equipped with such windings have been compared in [10], which showed that machines in which only alternate teeth are wound can offer significant performance advantages. This paper investigates the potential for further increasing the winding flux linkage in such machines by employing unequal tooth widths, the wound teeth being wider so that the coil pitch approaches the pole pitch, as illustrated in Fig. 1(c). In this way, as will be shown later, the coil flux linkage is maximized and, more significantly, the phase back-EMF waveform becomes more trapezoidal. In the design of the magnetic circuit for such machines, it is worth noting that: 1) due to the similar slot and pole numbers, the difference in width of adjacent teeth is usually relatively small, especially as the pole number is increased; 2) only half the coil flux in the wound teeth passes through adjacent teeth.; 3) the slot area remains largely unchanged and, hence, the allowable current den-
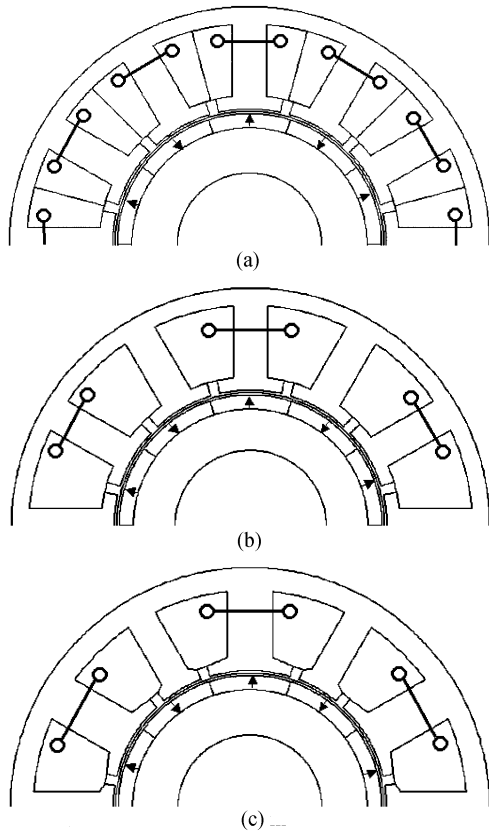
Fig. 1. Alternative winding configurations for 12-slot/ten-pole machines. (a) Machine A—all teeth wound. (b) Machine B—alternate teeth wound. (c) Machine C—alternate teeth wound on wider teeth.

Fig. 2. Schematic of phase windings. (a) Machine A. (b) Machines B and C.
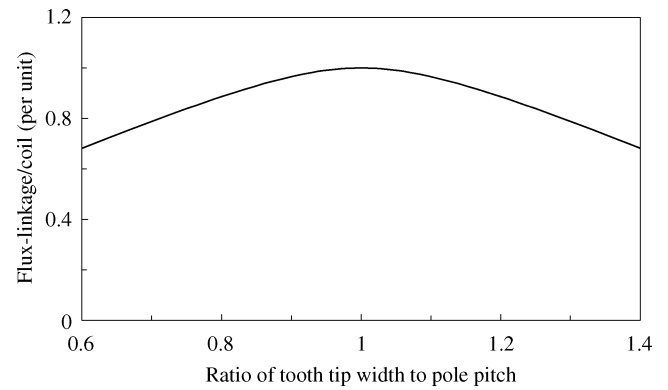
Fig. 3. Influence of coil pitch factor on flux linkage per coil.

TABLE I
MACHINE DIMENSIONS

	A	B	C
Active length (mm)	50	50	50
Stator outer diameter (mm)	100	100	100
Stator bore diameter (mm)	57	57	57
Stator yoke (mm)	3.7	3.7	4.8
Tooth width (mm)	7.1	7.1	9.5[a] 6.4[b]
Rotor outer diameter (mm)	49	49	49
Airgap length (mm)	1	1	1
Magnet thickness (mm)	3	3	3
Slot opening (mm)	2	2	2
Slot area (mm^2)	192	192	172
Slot packing factor	0.38	0.38	0.42
Phase resistance (mΩ)	300	350	360
Self inductance (mH)	3.03	4.64	4.94
Mutual inductance (mH)	-0.336	-0.002	-0.002

[a] teeth that carry a coil
[b] teeth that do not carry any coil

sity remains more or less the same; and 4) because of the increased width of the tooth tips of the wound teeth and the resulting increase in flux per tooth, the stator back iron is thicker.

III. MACHINE DIMENSIONS

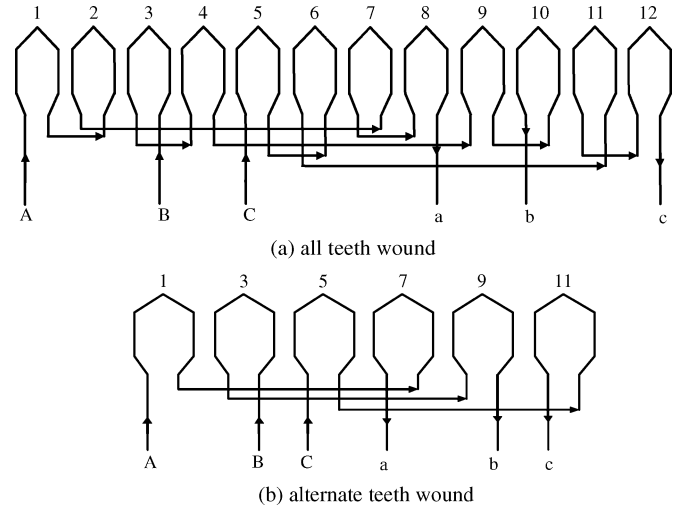The leading dimensions of the three machines shown in Fig. 1 are given in Table I, while schematics of their phase windings are shown in Fig. 2. In machine A, each stator slot accommodates two sides of two adjacent coils, and in a 12-slot/ten-pole machine four coils are connected in series to form a phase winding. In contrast, in machines B and C each phase winding only has half the number of coils, although the number of turns per coil is almost doubled in order to achieve the same EMF. However, each slot accommodates only one coil side, a significant advantage for fault-tolerant applications.

IV. INFLUENCE OF COIL PITCH FACTOR

The magnitude of the open-circuit flux which flows in a single tooth depends on the ratio of the width of the tooth tip to the pole pitch. Fig. 3 shows how the coil flux linkage varies with this ratio. Clearly, maximum flux linkage is achieved when the coil pitch factor is one, which corresponds to the slot number being equal to the pole number, i.e., $2p = N_s$, which is clearly impractical. However, machines in which $2p = N_s \pm 2$ can almost achieve unity coil pitch factor for maximum coil flux linkage by employing unequal tooth widths and dimensioning the tooth tips such that they approximately span one pole pitch.

V. FLUX LINKAGE AND PHASE BACK EMF

In two-dimensional (2-D) polar coordinates, and with due account of the influence of stator slotting, the air-gap flux density
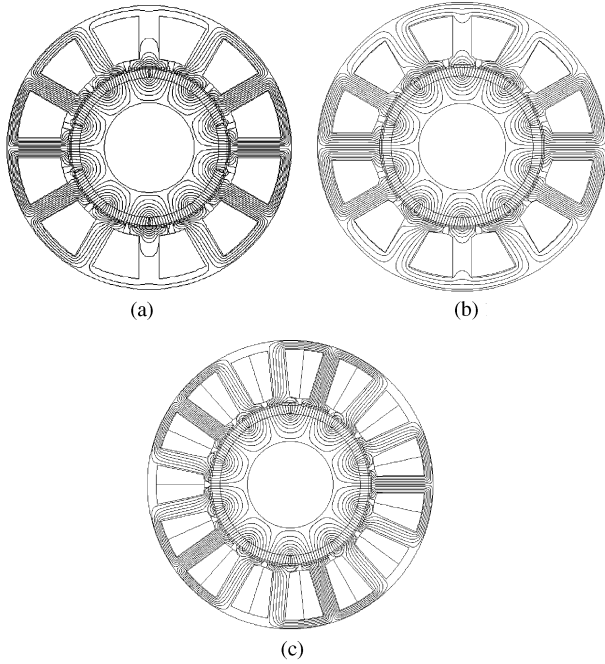
Fig. 4. Open-circuit field distributions in alternative machine designs. (a) 12-slot/ten-pole, equal tooth widths. (b) 12-slot/ten-pole, unequal tooth widths. (c) 15-slot/ten-pole, equal tooth widths.

distribution in a permanent-magnet machine equipped with a parallel magnetized surface-mounted magnet rotor can be expressed as [11]

$$B_{\text{airgap}}(r, \theta) = \sum_{n=1,3,5\ldots}^{\infty} B_n(r)\cos(np\theta) \cdot \lambda_{\text{rel}}(\theta) \quad (1)$$

where $B_n(r)$ depends on the pole number, the stator bore radius, the rotor outer radius and the magnet inner radius, as well as the harmonic orders, and $\lambda_{\text{rel}}(\theta)$ is the relative permeance function [11]. Finite-element predicted open-circuit field distributions for the 12-slot/ten-pole $(2p = N_s - 2)$ machines having equal and unequal tooth widths are shown in Fig. 4(a) and (b), respectively, while that for a conventional 15-slot/ten-pole $(N_s/2p = 3/2)$ machine is shown in Fig. 4(c). The air-gap flux-density distributions at the stator bore of the three machines have also been calculated analytically and compared with those obtained from finite-element analysis, as shown in Fig. 5.

The open-circuit flux linkage per coil is given by

$$\psi_{\text{coil}} = 2R_s l_a N_c \sum_{n=1,3,5\ldots}^{\infty} K_{pn} B_n(R_s)\cos(np\omega_r t) \quad (2)$$

where N_c, l_a, R_s, and ω_r are the number of turns per coil, the stator active axial length, the stator bore radius, and the rotor speed (rad/s), respectively. The coil pitch factor is given by $K_{pn} = \sin(np\pi/N_s)$ for the machines shown in Fig. 1(a) and (b), while for the machine shown in Fig. 1(c), i.e., 12-slot/ten-pole unequal tooth width machine, it is unity. The resulting flux-linkage waveforms are shown in Fig. 6. As can be seen, the 12-slot/ten-pole unequal tooth width machine exhibits the maximum flux linkage per coil, the flux linkage per coil in the 12-slot/ten-pole equal tooth width machine being slightly lower
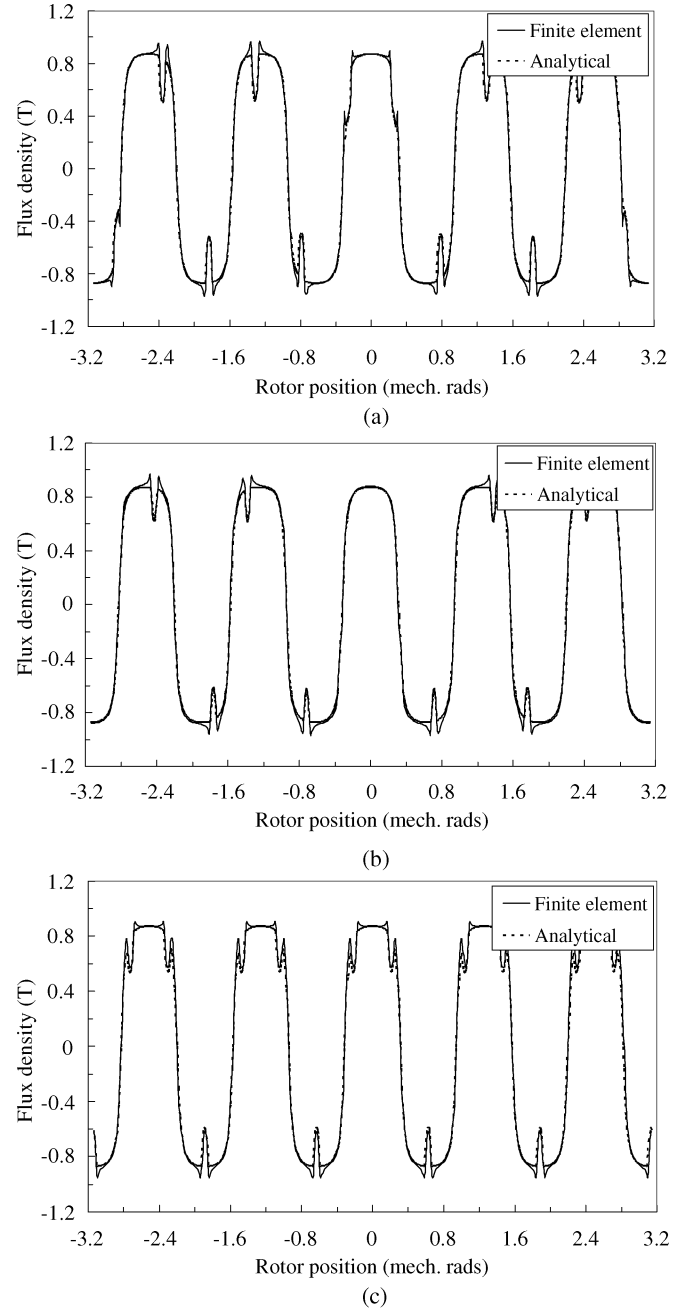

Fig. 5. Open-circuit flux density distributions. (a) 12-slot/ten-pole equal tooth widths. (b) 12-slot/ten-pole unequal tooth widths. (c) 15-slot/ten-pole equal tooth widths.

due to the smaller coil pitch factor, both being significantly higher than that for the 15-slot/ten-pole machine.

The phase back EMF, which results from the rate of change of flux linkage, can be expressed as

$$\text{EMF} = 2R_s l_a N_p \omega_r \sum_{n=1,3,5\ldots}^{\infty} K_{dpn} B_n(R_s)\sin(np\omega_r t) \quad (3)$$

where N_p and K_{dpn} are the number of turns per phase, and the winding factor, respectively. The back-EMF waveform is influenced by the winding factor K_{dpn} (the product of the coil pitch factor and coil disposition factor), which for the 12-slot/ten-pole machine in which all the teeth carry a coil is given by
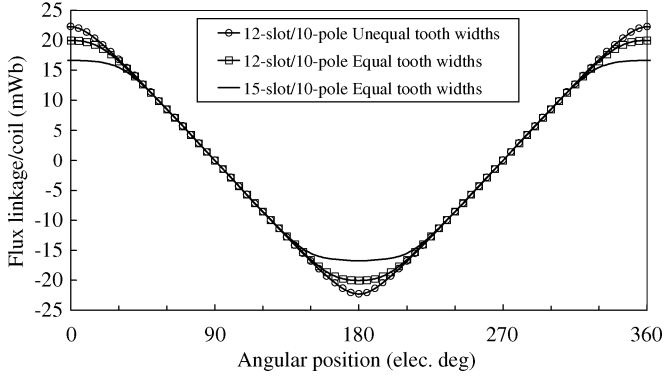
Fig. 6. Analytically predicted flux-linkage waveforms for alternative machine designs.

TABLE II
WINDING FACTOR K_{dpn}

	Harmonic order			
	n=1	n=3	n=5	n=7
12-slot/10-pole unequal tooth widths	1.0	1.0	1.0	1.0
12-slot/10-pole alternate teeth wound	0.966	0.707	0.259	0.259
12-slot/10-pole all teeth wound	0.933	0.500	0.067	0.067
15-slot/10-pole all teeth wound	0.866	0	0.866	0.866

TABLE III
AMPLITUDE OF FUNDAMENTAL AND HARMONIC PHASE BACK
EMF AT 400 r/min (V)

| Machines	Harmonic order			
	n=1	n=3	n=5	n=7
12-slot/10-pole unequal tooth widths	16.52	3.79	1.35	0.50
12-slot/10-pole alternate teeth wound	15.80	2.38	0.11	0.26
12-slot/10-pole all teeth wound	15.39	1.89	0.16	0.15
15-slot/10-pole all teeth wound	14.47	0	1.53	0.77

$K_{dpn} = \sin^2(np\pi/N_s)$, while for the 12-slot/ten-pole machine in which only alternate teeth are wound, and for the 15-slot/ten-pole machine, $K_{dpn} = \sin(np\pi/N_s)$. Tables II and III show the winding factor and the amplitude of the fundamental and harmonic phase back EMFs for the various machines. The lowest amplitude and the least trapezoidal phase EMF waveform results with the 15-slot/ten-pole motor due to the much bigger difference between the slot pitch and pole pitch. Hence, it has the smallest winding factor. The 12-slot/ten-pole machine with unequal tooth widths, for which $K_{dpn} = 1$, has the highest amplitude EMF. It also has the most trapezoidal phase back-EMF waveform (Figs. 7 and 8), which make it most appropriate for brushless dc operation.

VI. WINDING INDUCTANCES AND COGGING TORQUE

The winding arrangement obviously has a significant influence on the self- and mutual inductances. For example, in the 12-slot/ten-pole machine A in which all the teeth are wound, the winding disposition is A′ACC′B′BAA′C′CBB′, and the self-
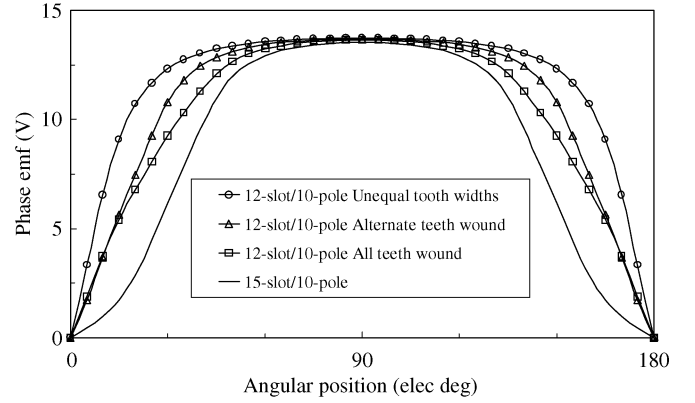
(a)
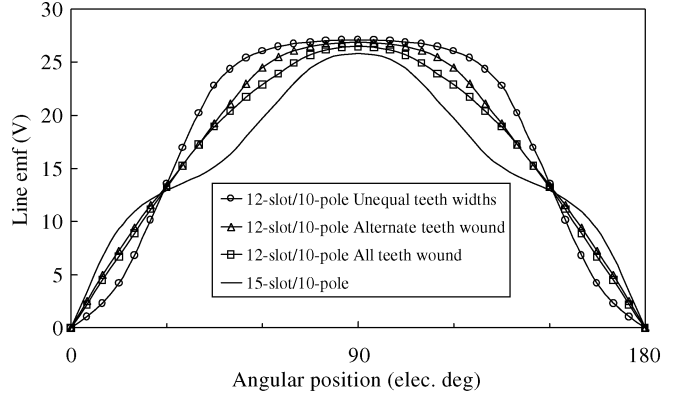
(b)

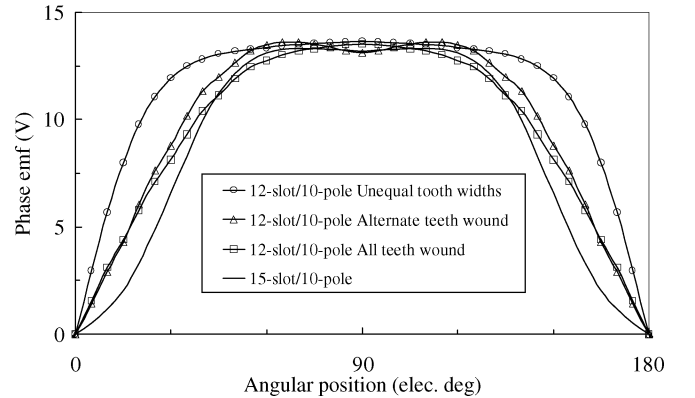Fig. 7. Analytically predicted phase and line EMF waveforms. (a) Phase EMF. (b) Line EMF.

Fig. 8. Finite-element predicted phase EMF waveforms.

and mutual inductances are 3.303 and −0.336 mH, respectively. For the machines in which only alternate teeth carry a coil, the winding disposition is A B′ C A′ B C′, and the self- and mutual inductances are 4.64 and −2.25 μH, respectively, for machine B, and 4.94 and −2.23 μH, respectively, for machine C.

Machines for which $2p = N_s \pm 2$ generally exhibit a very low cogging torque since the ratio of the slot number to pole number is fractional and the smallest common multiple N_{scm} between the slot number and pole number is high [12]. Fig. 9 shows predicted cogging torque waveforms, the analytical results being based on the method presented in [12]. For the 15-slot/ten-pole machine, $N_{scm} = 30$, while $N_{scm} = 60$ for the 12-slot/ten-pole machines. Thus, the cogging torque is ∼11% of the rated torque for the 15-slot/ten-pole machine, and this

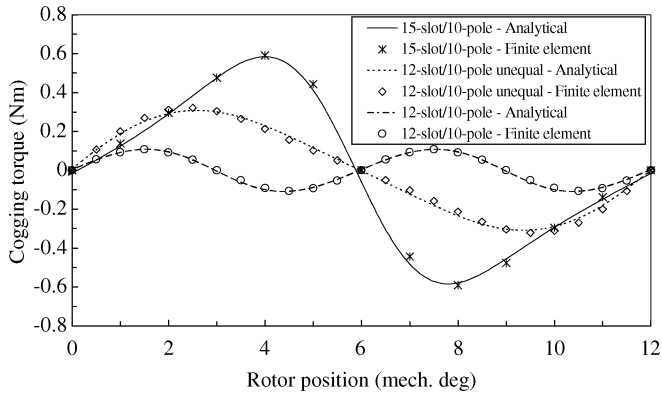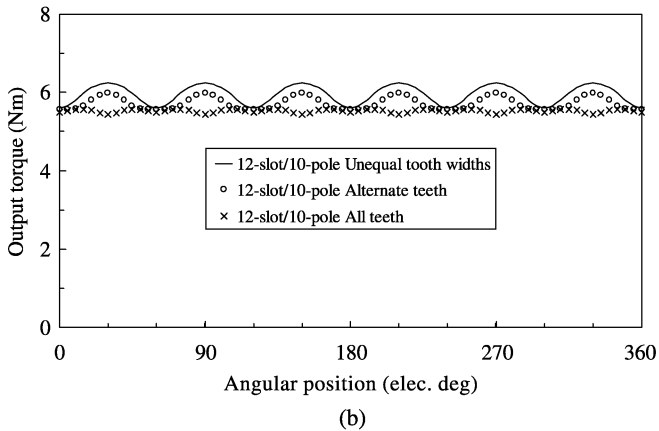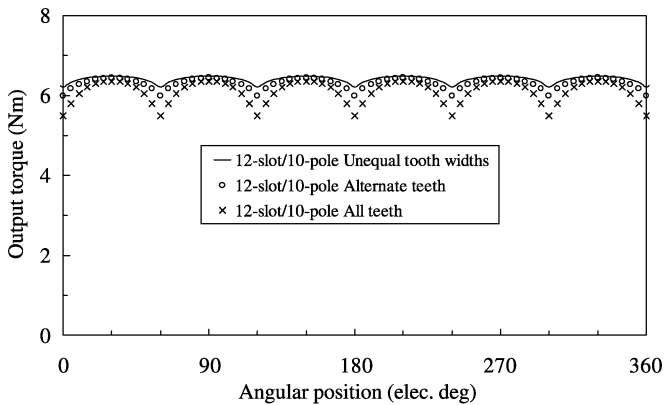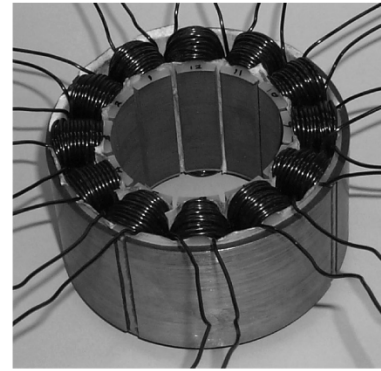Fig. 9.   Predicted cogging torque waveforms.

(a)

(b)

Fig. 10.   Analytically predicted electromagnetic torque. (a) Torque output with rectangular current waveform. (b) Torque output with sinusoidal current excitations.

Fig. 11.   Prototype 12-slot/ten-pole machines. (a) All teeth wound. (b) Alternate teeth wound. (c) Unequal tooth widths. (d) Rotor.

reduces to ∼2% and 5%, respectively, for the 12-slot/ten-pole machine with equal tooth widths and the 12-slot/ten-pole machine with unequal tooth widths.
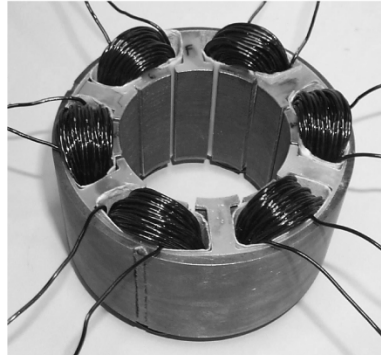
VII. ELECTROMAGNETIC TORQUE AND TORQUE RIPPLE

The instantaneous electromagnetic torque for either brushless dc or ac operation can be calculated from
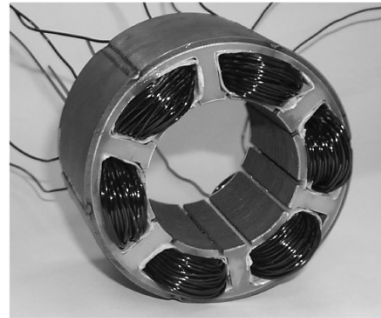
$$T_{\text{inst}} = \frac{1}{\omega_r}(e_a i_a + e_b i_b + e_c i_c) \qquad (4)$$

where e_a, e_b, e_c, i_a, i_b, and i_c are the instantaneous back EMFs and currents in phases A, B, and C, respectively. When the three 12-slot/ten-pole motors which have been considered in this paper are supplied with 120° rectangular current waveforms (10-A amplitude), i.e., brushless dc operation, the predicted output torque waveforms are as shown in Fig. 10(a). Clearly, since motor C has the most trapezoidal phase back-EMF waveform, it has a higher torque capability as well as a significantly lower torque ripple.

When the three machines are supplied with sinusoidal current waveforms, the 12-slot/ten-pole machine in which all the teeth are wound exhibits a very low torque ripple, as shown in
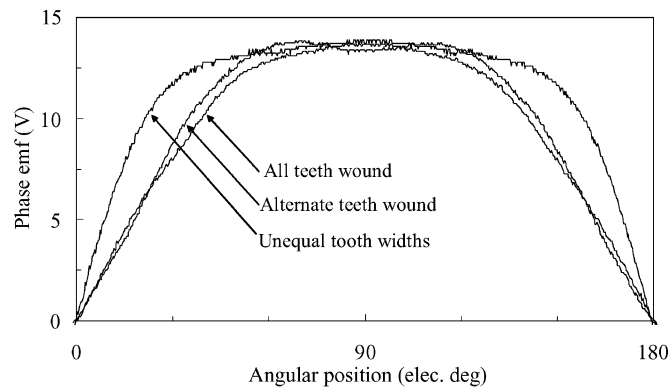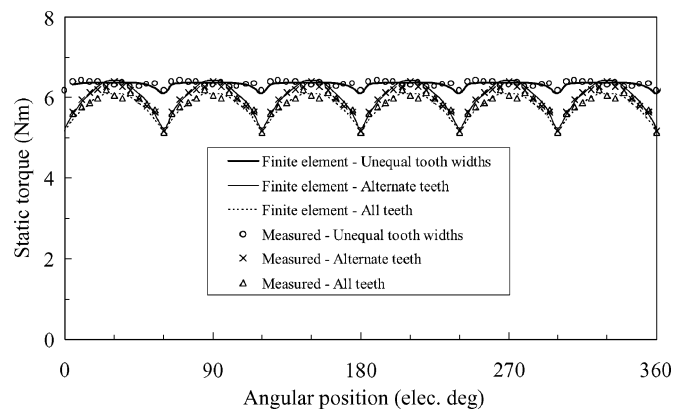
Fig. 12.   Measured phase EMF waveforms.

Fig. 13.   Measured and finite-element predicted static torque waveforms.
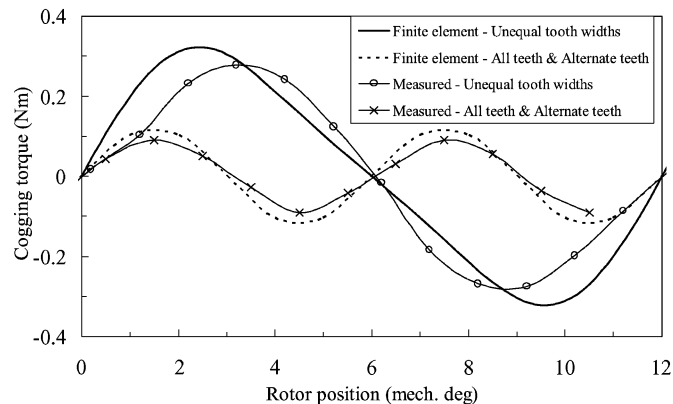

Fig. 14.   Measured and finite-element predicted cogging torque waveforms.

TABLE IV
MEASURED AND FINITE-ELEMENT PREDICTED SELF- AND MUTUAL
INDUCTANCES OF 12-SLOT/TEN-POLE MACHINES

Inductances (mH)	All teeth		Alternate teeth		Unequal tooth widths	
	Meas.	Pred.	Meas.	Pred.	Meas.	Pred.
Self-inductance	2.91	3.3	4.62	4.6	4.85	4.94
Mutual-inductance	-0.32	-0.33	-0.01	-0.00225	-0.001	-0.0023

torque characteristics for the three machines when two phase windings are excited with a dc current of 10 A, while the measured cogging torque waveforms are shown in Fig. 14, and measured self- and mutual inductances are given in Table IV. Again, all the measurements are in excellent agreement with analytical and/or finite-element predictions.

IX. CONCLUSION

The performance of alternative designs of three-phase permanent-magnet brushless machines which have nonoverlapping stator windings has been investigated. It has been shown that machines which have $2p = N_s \pm 2$ and unequal tooth widths can offer useful performance benefits, in terms of a higher torque capability and reduced torque ripple.

REFERENCES

[1] R. Mizutani and N. Matsui, "Optimum design approach for low-speed, high-torque permanent magnet machines," *Elect. Eng. Jpn.*, vol. 135, no. 4, pp. 52–63, 2001.
[2] C. C. Chan, J. Z. Jiang, G. H. Chen, X. Y. Wang, and K. T. Chau, "A novel polyphase multipole square-wave permanent magnet machine drive for electric vehicles," *IEEE Trans. Ind. Appl.*, vol. 30, no. 5, pp. 1258–1266, Sep./Oct. 1994.
[3] A. G. Jack, B. C. Mecrow, and J. A. Haylock, "A comparative study of permanent magnet and switched reluctance machines for high-performance fault-tolerant applications," *IEEE Trans. Ind. Appl.*, vol. 32, no. 4, pp. 889–895, Jul./Aug. 1996.
[4] B. C. Mecrow, A. G. Jack, and J. A. Haylock, "Fault tolerant permanent magnet machine drives," in *Proc. IEE Conf. Electrical Machines and Drives*, 1995, pp. 433–437.
[5] T. Gopalarathnam, H. A. Toliyat, and J. C. Moreira, "Multi-phase fault-tolerant brushless DC machine drives," in *Conf. Rec. IEEE-IAS Annu. Meeting*, vol. 3, 2000, pp. 1683–1688.
[6] J. D. Ede, K. Atallah, and D. Howe, "Design variants of modular permanent magnet brushless machine," *J. Appl. Phys.*, vol. 91, no. 10, pp. 6973–6975, 2002.
[7] T. Koch and A. Binder, "Permanent magnet machines with fractional slot winding for electric traction," in *Proc. ICEM'02*, Brugge, Belgium, Aug. 2002, CD-ROM.
[8] J. Cros and P. Viarouge, "Synthesis of high performance PM motors with concentrated windings," *IEEE Trans. Energy Convers.*, vol. 17, no. 2, pp. 248–253, Jun. 2002.
[9] D. Ishak, Z. Q. Zhu, and D. Howe, "High torque density permanent magnet brushless machines with similar slot and pole numbers," in *Proc. Int. Conf. Magnetism*, Rome, Italy, 2003, p. 536.
[10] ——, "Comparative study of permanent magnet brushless machines with all teeth and alternate teeth windings," in *Proc. IEE 2nd Int. Conf. Power Electronics, Machines and Drives*, 2004, pp. 834–839.
[11] Z. Q. Zhu, D. Howe, and C. C. Chan, "Improved analytical model for predicting the magnetic field distribution in brushless permanent-magnet machines," *IEEE Trans. Magn.*, vol. 38, no. 1, pp. 229–238, Jan. 2002.
[12] Z. Q. Zhu and D. Howe, "Influence of design parameters on cogging torque in permanent magnet machines," *IEEE Trans. Energy Convers.*, vol. 15, no. 4, pp. 407–412, Dec. 1992.

Fig. 10(b), since its phase back EMF has a relatively low harmonic content. However, the 12-slot/ten-pole machine in which only alternate teeth are wound and has unequal tooth widths exhibits the highest torque, albeit with the highest torque ripple.

VIII. EXPERIMENTAL VALIDATION

Fig. 11 shows the stators of three prototype 12-slot/ten-pole motors, together with a rotor. Fig. 12 shows the measured phase back-EMF waveforms, which are in good agreement with the predictions given in Figs. 7 and 8. Fig. 13 shows measured static

Dahaman Ishak received the B.Eng. degree from Syracuse University, Syracuse, NY, in 1990, and the M.Sc. degree from the University of Newcastle upon Tyne, Newcastle, U.K., in 2001, both in electrical engineering. He is currently working toward the Ph.D. degree in the Department of Electronic and Electrical Engineering, University of Sheffield, Sheffield, U.K., working on the design and analysis of low-speed high-torque permanent-magnet brushless machines.
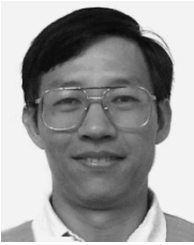
Z. Q. Zhu (M'90–SM'00) received the B.Eng. and M.Sc. degrees from Zhejiang University, Hangzhou, China, in 1982 and 1984, respectively, and the Ph.D. degree from the University of Sheffield, Sheffield, U.K., in 1991, all in electrical and electronic engineering.

From 1984 to 1988, he lectured in the Department of Electrical Engineering, Zhejiang University. Since 1988, he has been with the University of Sheffield, where he is currently a Professor of Electronic and Electrical Engineering. His current major research interests include applications, control, and design of permanent-magnet machines and drives.

Prof. Zhu is a Chartered Engineer in the U.K. and a Member of the Institution of Electrical Engineers, U.K.

David Howe received the B.Tech. and M.Sc. degrees from the University of Bradford, Bradford, U.K., in 1966 and 1967, respectively, and the Ph.D. degree from the University of Southampton, Southampton, U.K., in 1974, all in electrical power engineering.

He has held academic posts at Brunel and Southampton Universities, and spent a period in industry with NEI Parsons Ltd., working on electromagnetic problems related to turbogenerators. He is currently a Professor of Electrical Engineering at the University of Sheffield, Sheffield, U.K., where he heads the Electrical Machines and Drives Research Group. His research activities span all facets of controlled electrical drive systems, with particular emphasis on permanent-magnet excited machines.

Prof. Howe is a Chartered Engineer in the U.K., and a Fellow of the Institution of Electrical Engineers, U.K., and the Royal Academy of Engineering.